Acta Crystallographica Section D
Biological Crystallography
ISSN 0907-4449

Structure of the functional domain of the major grass-pollen allergen Phlp 5b

Kanagalaghatta Rajashankar,[a]†‡ Albrecht Bufe,[b]‡ Wolfgang Weber,[a]‡ Susanne Eschenburg,[a] Buko Lindner[c] and Christian Betzel[a]*

[a]Institut für Medizinische Biochemie und Molekularbiologie, Universitätsklinikum Hamburg-Eppendorf, c/o DESY, Gebäude 22a, Notkestrasse 85, 22603 Hamburg, Germany, [b]Experimentelle Pneumologie, Ruhr-Universität Bochum, 44789 Bochum, Germany, and [c]Medizinische und Biochemische Mikrobiologie, Forschungszentrum Borstel, 23845 Borstel, Germany

† Present address: Brookhaven National Laboratory, Building 725A-X9, Upton, NY 11973, USA.
‡ KR, AB and WW contributed equally to this publication.

Correspondence e-mail: betzel@unisgi1.desy.de

© 2002 International Union of Crystallography
Printed in Denmark – all rights reserved

Received 29 November 2001
Accepted 19 April 2002

PDB Reference: [Phlp 5b]', 1l3p.

The major allergen Phlp 5b from timothy grass pollen induces allergic rhinitis and bronchial asthma in millions of allergic patients worldwide. As an important step towards understanding the interactions between the pollen protein and components of the human immune system, the structure of the C-terminal key domain of Phlp 5b has been determined at 2.0 Å resolution and refined to an R value of 19.7%. This is the first known allergen composed entirely of α-helices. The protein forms a dimer stabilized by one intermolecular disulfide bridge. Sequence homology suggests that at least all group V and group VI grass-pollen allergens belong to this new class of 'four-helix-bundle allergens'.

1. Introduction

Allergic diseases are increasing worldwide and impose a huge burden on westernized societies. The physiological as well as the structural mechanism of allergy is deeply complex and the individual steps of molecular recognition are understood only very preliminarily (Rouvinen *et al.*, 1999; Suphioglu *et al.*, 1997). Allergies are induced by various compounds defined as allergens and once patients produce specific immunglobulin E (IgE) antibodies against these molecules they are sensitized. This situation is characterized by a predominance of T-helper 2 cells (Th2), mainly producing various cytokines such as IL-4, IL-5 and IL-13 (Suphioglu *et al.*, 1997; Burney *et al.*, 1997; Beasley, 1998; Vercelli *et al.*, 1998; Romagnani, 1997). IL-4 is the most prominent of these cytokines promoting IgE production. Effector cells (*i.e.* mast cells) in the mucosa or skin are coated with these IgE antibodies *via* high-affinity Fc receptors and are thus prepared to encounter the allergen. If this occurs and if at least two IgE antibodies are crosslinked *via* epitopes on the surface of the allergen, a release of mediators is induced, leading ultimately to the allergic inflammation (Sutton & Gould, 1993). About half of all allergic patients are sensitized towards grass-pollen proteins. Phlp 5b (derived from *Phleum pratense*, timothy grass) is one of the most relevant of these molecules and causes allergies in the majority of sensitized patients (Wissenbach *et al.*, 1998). No specific features of these molecules have been identified so far that explain why these pollen-protein molecules induce an allergic inflammatory response. While considerable knowledge of the primary structures of allergens has been gathered, analysis of their three-dimensional structures has started only recently with the application of X-ray crystallography and nuclear magnetic resonance spectroscopy. Today, several three-dimensional structures of allergenic molecules have been published: they were determined by comparative modelling (Baur *et al.*, 1986; Topham *et al.*, 1994), by NMR

(Metzler *et al.*, 1992; Faber *et al.*, 1996; Ichikawa *et al.*, 1998,), by X-ray crystallography (Rouvinen *et al.*, 1999; Fedorov, Ball, Mahoney *et al.*, 1997; Fedorov, Ball, Valenta *et al.*, 1997; Thorn *et al.*, 1997; Bocskei *et al.*, 1992; Brownlow *et al.*, 1997; Lascombe *et al.*, 2000; Mirza *et al.*, 2000) and by combined NMR and X-ray crystallography (Gajhede *et al.*, 1996; Faber *et al.*, 1996). Although a predominant β-sheet content is noticeable in the published structures (Rouvinen *et al.*, 1999), specific structural features explaining the allergenicity of these proteins have not been identified. Nevertheless, since it is ultimately the three-dimensional structure which determines the interaction of allergen and IgE antibodies, further structural knowledge is necessary to understand the phenomenon of allergenicity. Therefore, we have applied X-ray crystallographic methods in order to determine the structure of the pollen allergen Phlp 5b. In a first attempt to crystallize the entire 29 kDa allergen Phlp 5b, we observed limited proteolysis of the holoprotein to a mixture of several fragments from which one particular polypeptide preferentially crystallized (Bufe *et al.*, 1996). It was identified as a 13 kDa C-terminal fragment, here termed [Phlp 5b]′, which turned out to possess the full allergenic activity of the parental Phlp 5b. The observation that a similar fragment is produced from Phlp 5b in the presence of human mucosa (Bufe *et al.*, 1998) leads to the conclusion that it represents the biologically and clinically important domain of the major grass-pollen allergen Phlp 5b.

2. Material and methods

Recombinant [Phlp 5b]′ was cloned, expressed and purified as described in Bufe *et al.* (1996). Crystals were grown using the vapour-diffusion technique by mixing 2 µl of the protein solution at a concentration of 6 mg ml^{-1} and 2 µl of 1.6 *M* phosphate pH 4.0 containing 0.5 m*M* $MgCl_2$/0.1 m*M* ATP as a precipitant. Orthorhombic crystals with dimensions of 0.2 × 0.2 × 0.4 mm grew within 5 d at 295 K.

Analysis of crystals by matrix-assisted laser desorption/ionization mass spectrometry (MALDI–MS) of allergen samples was performed using a Bruker-Reflex III instrument (Bruker–Franzen Analytik, Bremen, Germany) in linear TOF configuration at an acceleration voltage of 20 kV and with delayed ion extraction. [Phlp 5b]′ was dissolved in water at a concentration of 7 µg µl^{-1}, further diluted in the ratio 1:60 with a freshly prepared matrix solution [saturated 3,5-dimethoxy-4-hydroxycinnamic acid (sinapic, SA; Aldrich) in a 2:1 mixture of 0.1% trifluoroacetic acid/acetonitrile]. 0.5 µl aliquots were deposited on a metallic sample holder and analyzed immediately after drying in a stream of air. Mass-scale calibration was performed internally by adding the appropriate amounts of insulin and cytochrome *c* (Sigma). Three crystals were washed with 2 *M* ammonium sulfate pH 4 and redissolved in 200 µl water; a 10 µl aliquot mixed with matrix solution in a ratio of 1:9 was further treated as described before.

Native diffraction data to high resolution were collected using synchrotron radiation at beamline BW6 (DESY, Hamburg) equipped with a MAR image-plate scanner and applying cryoconditions using 22% ethylene glycol in the mother liquor as cryoprotectant. The images were processed using *DENZO* and *SCALEPACK* (Otwinowski & Minor, 1997). The space group was assigned to be $C222_1$, with unit-cell parameters a = 38.97, b = 50.36, c = 107.80 Å and one molecule of [Phlp 5b]′ in the asymmetric unit. The calculated Matthews coefficient (Matthews, 1968) is 2.24 Å^3 Da^{-1}, which corresponds to a solvent-volume fraction of approximately 50%. The data-collection and refinement statistics are summarized in Table 1. One heavy-atom derivative was prepared by soaking native crystals of [Phlp 5b]′ for 36 h at 289 K in a 1 m*M* $HgCl_2$ solution containing 2 *M* phosphate buffer pH 4.5. Derivative data to 3.0 Å were collected using a Rigaku rotating-anode generator equipped with a MAR image plate and processed accordingly. The *CCP*4 program suite (Collaborative Computational Project, Number 4, 1994) was used for most calculations. One major site and two minor sites were identified by the difference Patterson methods and three additional minor sites were located in the difference Fourier maps. Heavy-atom parameters were refined to 3.8 Å

Table 1
Summary of data collection, phasing and structure-refinement parameters.

Crystal	Native	$HgCl_2$ derivative
Data collection		
X-ray source	Synchrotron	Rotating anode
Wavelength (Å)	1.2	1.54182
Max. resolution (Å)	1.98	3.0
Total No. of reflections	56414	21235
No. of unique reflections	7641	2242
Unique reflections (>1σ) (%)	96.5 (92.1)	86.1 (92.9)
Completeness (%)	99.6 (98.7)	91.5 (99.6)
R_{sym}†	4.1	11.8
Phasing		
Resolution range (Å)	25.0–3.8	
No. of sites‡ (major/minor sites)	6 (1/5)	
R_{cullis}§ (centric/acentric)	0.40/0.52	
R_{cullis} (anomalous)	0.90	
Phasing power¶ (centrics/acentrics)	2.5/2.4	
Figure of merit (SIR)	0.55	
Figure of merit (after density modification)	0.75	
Refinement		
Resolution range (Å)	27.0–1.98	
R factor††/R_{free}‡‡	19.7/24.1	
No. of protein atoms	738	
No. of solvent molecules	97	
Average B factor (Å^2)		
All atoms	20.2	
Main-chain atoms	17.5	
Side-chain atoms	20.9	
R.m.s. deviations		
Bonds (Å)	0.011	
Angles (°)	1.3	
Torsions (°)	21.3	

† $R(I) = \sum |I - \langle I \rangle| / \sum (I)$, where I is the intensity of a given reflection and $\langle I \rangle$ is the average intensity for multiple measurements of this reflection. ‡ The relative occupancies (anomalous occupancies in parentheses) of these sites are 0.49 (0.49), 0.17 (0.15), 0.14 (0.18), 0.19 (0.10), 0.11 (0.10) and 0.04 (0.04). § $R_{cullis} = \sum \big| |F_{PH}| \pm |F_P| \big| - |F_H| \big| / \sum \big| |F_{PH}| \pm |F_P| \big|$, where F_H is the calculated heavy-atom structure factor. ¶ Phasing power = r.m.s. of ($|F_H|/E$), where E is the residual lack-of-closure error. †† R factor = $\sum \big| |F_{obs}| - |F_{calc}| \big| / \sum |F_{obs}|$, where F_{obs} and F_{calc} are the observed and calculated structure factors, respectively. ‡‡ R_{free} was calculated using 5% of the diffraction data that were selected randomly and not used throughout refinement.

using the program *MLPHARE* (Collaborative Computational Project, Number 4, 1994). The application of anomalous data from the mercury derivative complemented the phasing procedure. The backbone of the molecule was initially traced using solvent-flattened and phase-extended electron density (Cowtan, 1994). Phases calculated from the first model were combined with SIRAS phases. The resulting combined electron-density map exhibited density even for some of the bulky hydrophobic side chains; most of the side chains were modelled at this stage. Cycles of phase-combination model building and refinement resulted in the final model. This model was further refined using *X-PLOR* (Brünger, 1992). All data in the range 27–1.98 Å (except the $R_{\rm free}$ set) were used for the refinement without a σ-cutoff. Bulk-solvent correction was applied. The final model of [Phlp 5b]′ consists of 102 amino-acid residues and 97 water molecules. According to the electron density, one water molecule was reassigned as an Mg^{2+}, which was an ingredient of the precipitant solution, and one partially occupied phosphate group was identified. All residues have well defined electron density, as shown for example in Fig. 1, except the side chains of the three glutamines 145, 204 and 240. The N-terminal residue Lys138 is disordered. The final R factors are R = 19.7% and $R_{\rm free}$ = 24.1%, respectively. The model is characterized by stereochemical parameters well within acceptable ranges as analyzed by the program *PROCHECK* (Laskowski *et al.*, 1993). All residues fall into the allowed regions of the Ramachandran plot.

3. Results and discussion

Phlp 5b exhibits an entirely α-helical structure with a right-handed up–down–up–down four-helical bundle topology (Fig. 2*a*). The four helices, labelled *A*, *B*, *C* and *D*, are composed of residues 152–173, 177–195, 207–220 and 225–240, respectively (residue numbering according to PubMed Protein Database entry Q40963, 15 July 1999). Helices *A* and *B* are more amphiphilic than the other two. Helix *A* is bent at the N-terminal part and helix *D* is slightly extended. The four-helical bundle is characterized by inter-helical angles of 143 (*A*–*B*), 170 (*B*–*C*), 149 (*C*–*D*) and −148° (*A*–*D*), respectively, calculated using the program *HELIXANG* (Collaborative Computational Project, Number 4, 1994). The helices are connected by short linker segments 174–176 (*AB* linker), 196–206 (*BC* linker) and 221–224 (*CD* linker). The *AB* and *CD* linkers are composed of tight turns. The *BC* linker is

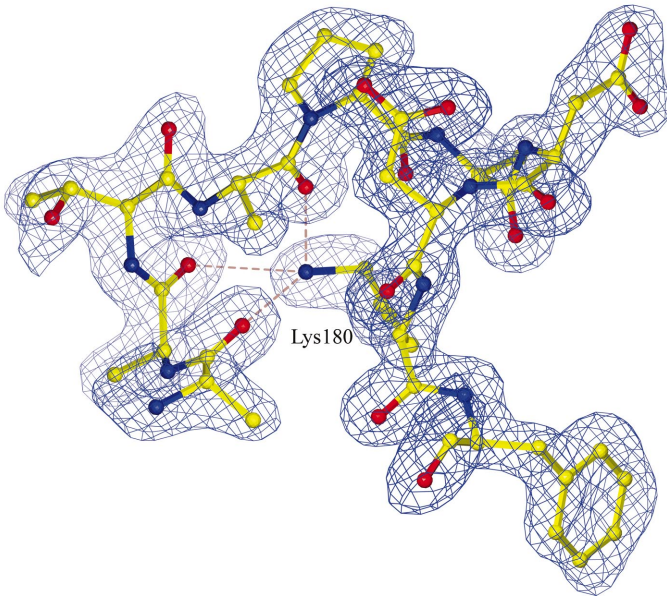

Figure 1
Final $2F_o - F_c$ electron-density map, contoured at the 1.4σ level, for residues 172–181 which represent the *AB* linker region. The lysine residue stabilizing the helix–turn–helix motif is labelled. Dashed lines indicate hydrogen bonds.

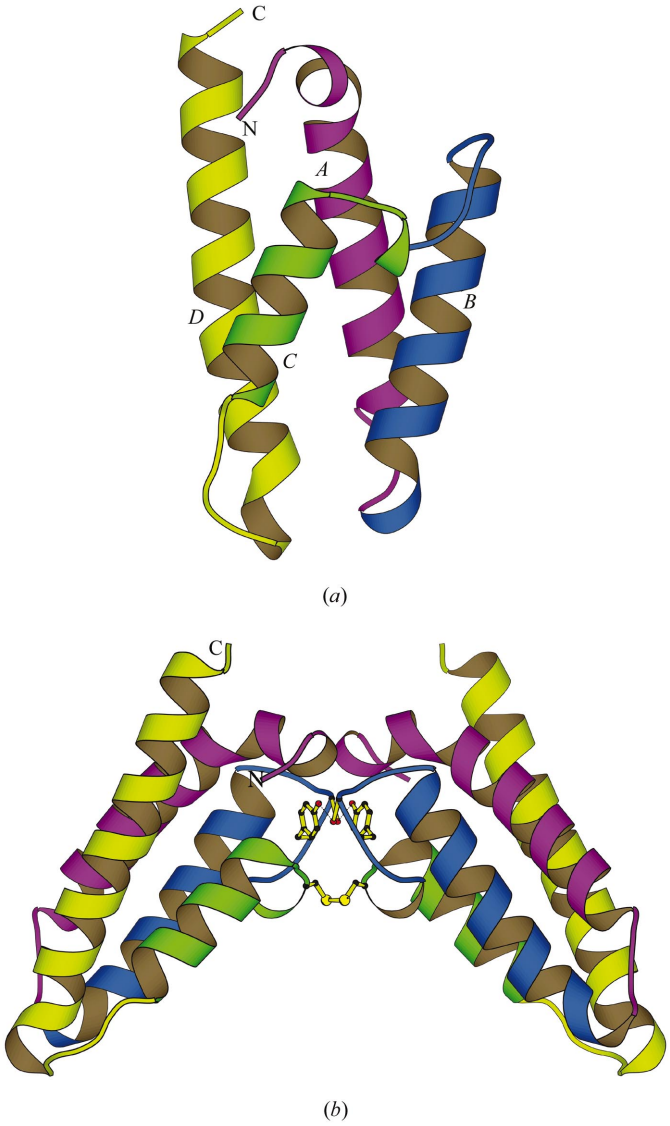

Figure 2
(*a*) The right-handed up–down four-helical bundle structure of [Phlp 5b]′ is shown as a ribbon cartoon. The N- and C-termini as well as the helices *A*, *B*, *C* and *D* are labelled. The helices are shown in four different colours. The figure was generated by *MOLSCRIPT* (Kraulis, 1991). (*b*) The crystallographic dimer of [Phlp 5b]′ is shown. The disulfide bridge and the two Tyr residues supporting the dimer formation are indicated in ball-and-stick format.

expanded and involves an incipient helical conformation for residues 202–204. The curvature of helix *A* is ~40° at the N-terminus. It is caused by a slight deviation from ideal α-helical values of the backbone dihedral angles of residues Glu154, Ile158 and Asp159 and by the interference of solvent waters with the typical hydrogen-bond structure. Helix *B* has the largest buried hydrophobic surface of the four. Furthermore, this helix is terminated by the so called 'Schellman motif', which is found to be a frequent mode of helix termination in proteins and synthetic peptides (Schellman, 1980). Gly197 adopts right-handed α-helical dihedral angles which favour the formation of the Schellman motif. Overall, the helical bundle buries 13 residues, forming a hydrophobic core. The residues involved in the core are Ile158, Ile161, Phe165, Phe181, Phe184, Phe188, Ile192, Ile206, Leu209, Val213, Phe232, Leu236 and Ile240. As expected, no polar or charged residues are buried in this region. This type of fold is different from all other allergen structures determined so far (Rouvinen *et al.*, 1999; Metzler *et al.*, 1992; Ichikawa *et al.*, 1998; Fedorov *et al.*, 1997; Gajhede *et al.*, 1996) and also different from those observed in numerous other four-helix-bundle proteins such as phospholipase C and several cytokines. A topology similar to that of Phlp 5b is found for cytochrome c' which, following the taxonomy of Harris *et al.* (1994), is classified as a 'square bundle'.

As shown in Figs. 2(*b*) and 3, the protein forms a stable dimer with a crystallographically twofold-related molecule which can be expected to be the stable physiologically active form. The dimer is stabilized by one intermolecular disulfide bridge between the twofold-related Cys205 residues and by ten intermolecular hydrogen bonds, including four bonds mediated through water molecules. The dimer is additionally stabilized by the aromatic interaction between symmetry-related Tyr200 residues. It appears that the disulfide bridge is compulsory for the stabilization of the dimer. Upon dimer formation, a surface area of approximately 420 Å^2 of each monomer is buried, which is ~10% of the total accessible surface area of the monomer.

Although [Phlp 5b]′ has been expressed as a protein corresponding to the C-terminal 136 amino-acid residues of the holo-allergen, starting at Lys149, the crystal structure contains only 102 residues, ending at Ile240. In order to decide whether the lack of electron density for 33 amino acids at the C-terminus was a consequence of disorder of the structure or of the absence of this part of the polypeptide in the crystal, single crystals were dissolved in water and subjected to mass spectrometry. The mass spectrum of the protein preparation prior to crystallization showed two peaks at 13 401 and 26 798 Da, respectively, corresponding to the monomer and the dimer. The sample derived from the crystal showed peaks at 11 840 and 23 680 Da (data not shown). Obviously, a C-terminal truncation has occurred during the crystal-growth experiment, indicating another site of limited proteolysis in the allergen molecule. This is in accordance with electrophoretic data that allergen preparations contain such small fragments after prolonged storage. Whether the allergen Phlp 5b is truncated in an autoproteolytic reaction or owing to a putative contamination with proteases is not clear at present; the phenomenon is at least reproducible, since different preparations of the protein behave in the same way. The fact that the mass spectrum of the redissolved crystal shows mainly the dimer peak, in contrast to the starting preparation which shows monomer and dimer in comparable amounts, indicates that not only C-terminal truncation but also dimer formation precede crystal growth.

To exclude the possibility that the C-terminal truncation led to loss of allergenic activity, dissolved crystals were used in an *in vitro* bronchial provocation test on human bronchial mucosa in an *ex vivo* lung slices culture. Compared with the parental Phlp 5b, the C-terminal truncated allergen induced significant obstruction of the small airways, indicating a specific IgE-mediated reaction of the mucosa (data not shown).

When performing a self-sequence comparison of [Phlp 5b]′ it turned out that two stretches of 35 residues with 46% sequence identity could be aligned (Fig. 4*a*). This sequence homology is also reflected in the three-dimensional structure, where each sequence stretch forms a helix–turn–helix motif. The three-dimensional homology of both stretches is further demonstrated by an r.m.s. deviation of 0.8 Å for superposition of 35 C^{α} atoms as shown in Fig. 4(*b*). Also, the molecular interactions expressing helix termination and chain reversal in these helix–turn–helix motifs are remarkably similar. One example is illustrated in Fig. 5. The NZ atoms of Lys180 and Lys228 from the second helix interfere with the helix hydrogen bonds of the first helix in both cases. Furthermore, Phe184 and Phe232 participate in the helix–helix packing. In addition, the presence of Pro177 and Pro225 facilitate helix termination as well as chain reversal. Finally, the solvent-accessible surface areas of the corresponding residues in the two segments is comparable overall (Fig. 4*c*). This kind of internal homology points to a special type of four-helix bundle topology, which can be defined as twinned two-helix bundle. Interestingly, this motif also seems to be present in the N-terminal part of the 29 kDa holo-allergen, which is not part of the three-dimensional structure presented here. The alignment of the sequence of this portion of the molecule with that of [Phlp 5b]′ for the region defining the helix–turn–helix motifs reveals a 60% homology (Fig. 5). Most probably, the holo-protein is assembled of two parts, each holding a four-helix-bundle structure or two helix–turn–helix motifs. Whether the holo-allergen forms a two-domain structure with a helix bundle in each domain or one multi-helix bundle will be clear after the determination of the complete structure. The internal structural homology of the entire Phlp 5b molecule was confirmed by the fact that IgE antibodies, isolated by affinity adsorption to [Phlp 5b]′, also recognize the N-terminal portion of the holo-allergen (data not shown).

4. Conclusions

Here we describe for the first time the structure of the functional domain of the major allergen Phlp 5b analyzed to 2.0 Å resolution. We present a novel four-helix-bundle allergen

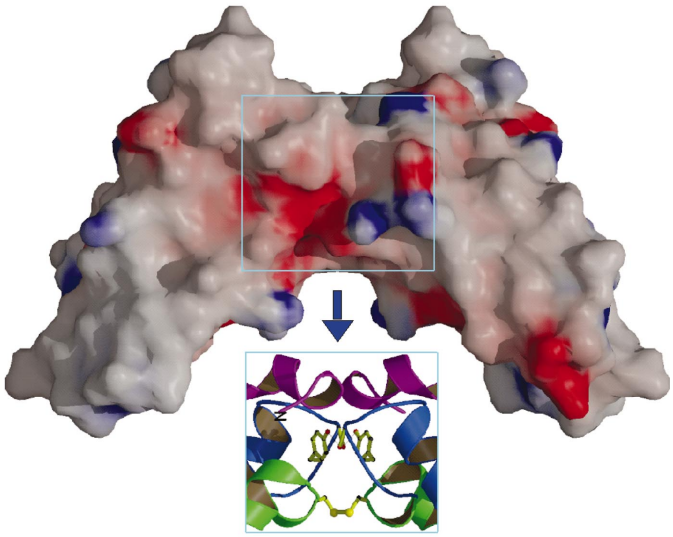

Figure 3
The molecular surface of the crystallographic dimer of [Phlp 5b]′ as created with the program *GRASP* (Nicolls *et al.*, 1991). Negative potentials are shown in red, positive potentials in blue. The inset indicates in a ball-and-stick representation the major interactions stabilizing the dimer: the disulfide bridge (Cys205 and symmetry-related Cys) and the two Tyr residues (Tyr200 and symmetry-related Tyr).

structure and it is reasonable to ask whether the structure can provide an explanation of the allergenic property of this molecule. An interpretation of allergenicity derived from three-dimensional structures has not so far been possible. The question is whether the structure of [Phlp 5b]′ allows identification of three-dimensional features of the IgE-binding epitopes that play a key role in evoking allergic symptoms. However, if we assign all peptide sequences known to bind IgE from various allergic patients (Schramm *et al.*, 2001), it becomes evident in the crystal structure of [Phlp 5b]′ that most parts of the allergen's surface can be potential candidates for recognition by IgE antibodies. Consequently, a common pattern for the three-dimensional architecture of IgE epitopes is not evident. A recent review of all known crystal structures of other allergens results in a similar conclusion (Rouvinen *et al.*, 1999). Nevertheless, the crystal structure of [Phlp 5b]′ points to a significant property which may be important for the allergenicity of this molecule. It is the compactness of the structure that confers conformational stability and may function as a 'shield' against proteolytic attack during the invasion of the allergen into the human tissue. The allergen has to overcome the proteolytic barrier of the respiratory mucosa with its conformation fully conserved before interacting with IgE antibodies. As it has turned out that IgE epitopes are mainly conformationally active, three-dimensional integrity is obviously essential for allergenicity. The presence of truncated Phlp 5b forms of about 11 kDa found in the nasal secretions of patients demonstrates that allergens are indeed subjected to proteolysis *in vivo* (Bufe *et al.*, 1998). The molecule described and discussed here is obviously generated by limited proteo-

```
IDKIDAAFKVAATAAATAPADDKFTVFEAAFNKAI  192
IPSLEAAVKQAYAATVAAAPQVKYAVFEAALTKAI  240
```

(*a*)

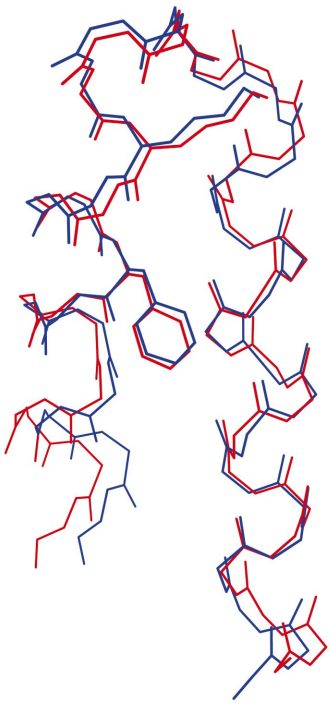

(*b*)

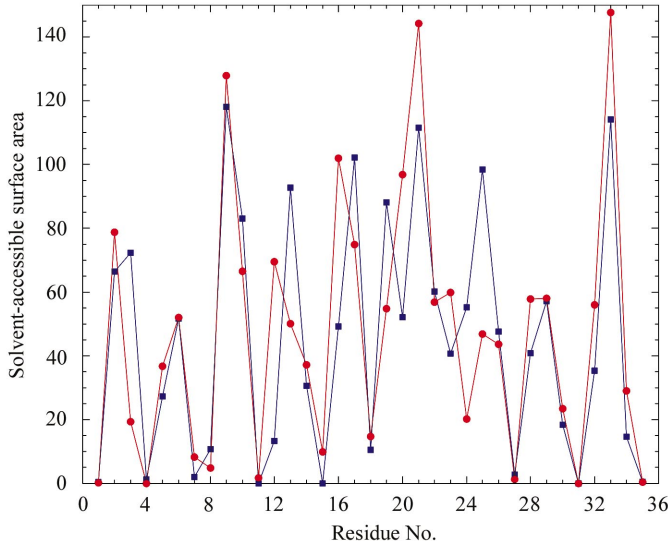

(*c*)

Figure 4
(*a*) Sequence alignment of the two 35-amino-acid stretches forming helix–turn–helix motifs in [Phlp 5b]′. The two segments 158–192 and 206–240 show an identity of 46%. Shaded boxes show identity (black) and homology (grey). (*b*) Three-dimensional superposition of the two 35-amino-acid stretches forming helix–turn–helix motifs in [Phlp 5b]′. The r.m.s. deviation for superpositioning 35 pairs of C^{α} atoms is 0.8 Å. Residues 158–192 and 206–240 are indicated in blue and red, respectively. The superposition was calculated using the program *O* (Jones *et al.*, 1991). (*c*) Solvent-accessible surface area for the 35-amino-acid stretches forming helix-turn-helix motifs in [Phlp 5b]′. The residues 158–192 and 206–240 are indicated in blue and red, respectively. The *x* axis shows the residue position and the *y* axis represents the solvent-accessible surface area in $Å^2$. The accessible surface areas were calculated using the program *NACCESS* (Hubbard & Thornton, 1993).

lysis of Phlp 5b *in vitro*. We have previously reported the preferential crystallization of a 13 kDa fragment (Bufe *et al.*, 1996) emerging from preparations of the 29 kDa parent protein by N-terminal truncation. The three-dimensional structure presented here reveals a further C-terminal truncation, resulting in a 11 kDa core domain. Whether these degradations are caused by endogenous or by contaminating proteolytic activities is not clear, but the stability of the 11 kDa four-helix bundle is obvious. The antiparallel orientation of the helices and relatively short linker segments provide compactness, which is the structural explanation for the domain integrity and is obviously essential for the preservation and donation of IgE-binding epitopes as a prerequisite of the allergenic effect.

While our data do not ultimately answer the question of what makes an antigen become an allergen, they do elucidate the minimum requirements for proteins to be allergenic. Finally, it can be proposed that allergens must contain at least one core domain which is stable towards proteolytic degradation and possesses high conformational integrity, thereby preserving the three-dimensional architecture of IgE-binding epitopes. The four-helix bundle of Phlp 5b apparently meets these requirements and survives as a compact structural unit after being truncated from the 29 kDa pollen protein and still exhibits full allergenicity (*in vitro* bronchial provocation test; data not shown). Thus, the four-helix bundle of Phlp 5b seems to represent the minimum possible structural unit for allergenicity. Furthermore, the structural symmetry of the homodimer and the internal sequence homology of the structural elements are probably connected with allergic effects.

When comparing the other available allergen structures reported so far, it is interesting to note that all of them are composed solely or at least mainly of β-structures (Rouvinen *et al.*, 1999). In contrast, the [Phlp 5b]′ structure presented here is the first example of an all-helical structure and may open up a new structural class of allergens. When looking for further candidates of this class of proteins it becomes obvious that the related isoallergens known from other grass species, such as rye grass, Kentucky bluegrass, canary grass and velvet grass, show considerable sequence homology (Petersen *et al.*, 1995; Suphioglu *et al.*, 1997; Gehlhar *et al.*, 1997). Therefore, it can certainly be assumed that they also contain the repetitive helix–turn–helix motif identified here for the first time in an allergen. In fact, it seems probable that group V and group VI grass-pollen allergens belong to this new class of allergens characterized by protease-resistant four-helix-bundle domains.

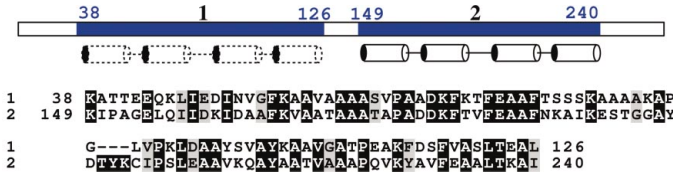

Figure 5
Self-sequence comparison of the entire Phlp 5b holoprotein. The holoprotein is made up of 284 amino acids, with two segments (blue regions; 1 and 2) showing a sequence homology of ~60%. The [Phlp 5b]′ four-helix-bundle structure corresponds to the C-terminal part of the holoprotein. The four helices representing this part are indicated schematically in bold. The sequence homology suggests that the N-terminal part also adopts a four-helix-bundle topology, indicated by dotted lines. The corresponding sequence alignment is shown below.

KRR thanks the Alexander-von-Humboldt Foundation for a Research Fellowship. This project was supported by the Deutsche Forschungsgemeinschaft (grants We 983/5-1, Bu 762/3-1) and the Deutsches Zentrum für Luft- und Raumfahrt (Grant 50 WB 9915).

References

Baur, X., Aschauer, H., Mazur, G., Dewair, M., Prelicz, H. & Steigemann, W. (1986). *Science*, **233**, 351–354.
Beasley, R. (1998). *Lancet*, **135**, 1225–1232.
Bocskei, Z., Groom, C. R., Flower, D. R., Wright, C. E., Phillips, S. E., Cavaggioni, A., Findlay, J. B. & North, A. C. (1992). *Nature (London)*, **360**, 186–188.
Brownlow, S., Morais Cabral, J. H., Cooper, R., Flower, D. R., Yewdall, S. J., Polikarpov, I., North, A. C. & Sawyer, L. (1997). *Structure*, **5**, 481–495.
Brünger, A. T. (1992). *X-PLOR, Version* 3.1. *A System for X-ray Crystallography and NMR.* New Haven, Connecticut: Yale University Press.
Bufe, A., Betzel, Ch., Schramm, G., Petersen, A., Becker, W.-M., Schlaak, M. & Weber, W. (1996). *J. Biol. Chem.* **271**, 27193–27196.
Bufe, A., Gehlhar, K., Schramm, G., Schlaak, M. & Becker, W. M. (1998). *Am. J. Respir. Crit. Care Med.* **157**, 1269–1276.
Burney, P., Malmberg, E., Chinn, S., Jarvis, D., Luczynska, C. & Lai, E. (1997). *J. Allergy Clin. Immunol.* **99**, 314–322.
Collaborative Computational Project, Number 4 (1994). *Acta Cryst.* D**50**, 760–763.
Cowtan, K. (1994). *Jnt CCP4/ESF–EACBM Newsl. Protein Crystallogr.* **31**, 34–83.
Faber, C., Lindemann, A., Sticht, H., Ejchart, A., Kungl, A., Susani, M., Frank, R. W., Kraft, D., Breitenbach, M. & Rosch, P. (1996). *J. Biol. Chem.* **271**, 19243–19250.
Fedorov, A. A., Ball, T., Mahoney, N. M., Valenta, R. & Almo, S. C. (1997). *Structure*, **5**, 33–45.
Fedorov, A. A., Ball, T., Valenta, R. & Almo, S. C. (1997). *Int. Arch. Allergy Immunol.* **113**, 109–113.
Gajhede, M., Osmark, P., Poulsen, F. M., Ipsen, H., Larsen, J. N. & Joost van Neerven, R. J. (1996). *Nature Struct. Biol.* **3**, 1040–1045.
Gehlhar, K., Petersen, A., Schramm, G., Becker, W. M., Schlaak, M. & Bufe, A. (1997). *Eur. J. Biochem.* **247**, 217–223.
Harris, N. L., Presnell, S. R. & Cohen, F. E. (1994). *J. Mol. Biol.* **236**, 1356–1368.
Hubbard, S. J. & Thornton, J. M. (1993). *NACCESS*. Department of Biochemistry and Molecular Biology, University College London, England.
Ichikawa, S., Hatanaka, H., Yuuki, T., Iwamoto, N., Kojima, S. & Nishiyama, C. (1998). *J. Biol. Chem.* **273**, 356–360.
Jones, T. A., Zou, J. Y., Cowan, S. W. & Kjeldgaard, M. (1991). *Acta Cryst.* A**47**, 110–119.
Kraulis, P. J. (1991). *J. Appl. Cryst.* **24**, 946–950.
Lascombe, M. B., Gregoire, C., Poncet, P., Tavares, G. A., Rosinski-Chupin, I., Rabillon, J., Goubran-Botros, H., Mazie, J. C., David, B. & Alzari, P. M. (2000). *J. Biol. Chem.* **275**, 21572–21577.
Laskowski, R. A., MacArthur, M. W., Moss, D. S. & Thornton, J. M. (1993). *J. Appl. Cryst.* **26**, 283–291.
Matthews, B. W. (1968). *J. Mol. Biol.* **33**, 491–497.
Metzler, W. J., Valentine, K., Roebber, M., Friedrichs, M. S., Marsh, D. G. & Mueller, L. (1992). *Biochemistry*, **31**, 5117–5127.

Mirza, O., Henriksen, A., Ipsen, H., Larsen, J. N., Wissenbach, M., Spangfort, M. D. & Gajhede, M. (2000). *J. Immunol.* **165**, 331–338.
Nicolls, A., Sharp, K. & Hornig, B. (1991). *Proteins Struct. Funct. Genet.* **11**, 281–296.
Otwinowski, Z. & Minor, W. (1997). *Methods Enzymol.* **276**, 307–326.
Petersen, A., Bufe, A., Schramm, G., Schlaak, M. & Becker, W. M. (1995). *Int. Arch. Allergy Immunol.* **108**, 55–49.
Romagnani, S. (1997). *Immunol. Today*, **18**, 263–266.
Rouvinen, J., Rautiainen, J., Virtanen, T., Zeiler, T., Kauppinen, J., Taivainen, A. & Mantyjarvi, R. (1999). *J. Biol. Chem.* **274**, 2337–2343.
Schellman, C. (1980). *Protein Folding*, edited by R. Jaenicke, pp. 53–61. Amsterdam: Elsevier.
Schramm, G., Bufe, A., Petersen, A., Haas, H., Merget, R., Schlaak, M. & Becker, W.-M. (2001). *Clin. Exp. Allergy*, **31**, 331–341.
Suphioglu, C., Onk, E. K., Knox, B. & Singh, M. B. (1997). *Allergens, Allergic Mechanisms and Immunotherapeutic Strategy*, p. 131. Chichester: John Wiley & Sons.
Sutton, B. J. & Gould, H. J. (1993). *Nature (London)*, **366**, 421–428.
Thorn, K. S., Christensen, H. E. M., Shigeta, R. Jr, Huddler, D. Jr, Shalaby, L., Lindberg, U., Chua, N.-H. & Schutt, C. E. (1997). *Structure*, **5**, 19–32.
Topham, C. M., Srinivasan, N., Thorpe, C. J., Overington, J. P. & Kalsheker, N. A. (1994). *Protein Eng.* **7**, 869–894.
Vercelli, D., De Monte, L., Monticelli, S., Di Bartolo, C. & Agresti, A. (1998). *Int. Arch. Allergy Immunol.* **116**, 1–4.
Wissenbach, M., Holm, J., van Neerven, R. J. J. & Ipsen, H. (1998). *Clin. Exp. Allergy*, **28**, 784–787.